Fuzzy-Adapted Recursive Sliding-Mode Controller Design for a Nuclear Power Plant Control

Zhengyu Huang, Robert M. Edwards, *Member, IEEE*, and Kwang Y. Lee, *Fellow, IEEE*

***Abstract*—In this paper, a multi-input multi-output fuzzy-adapted recursive sliding-mode controller (FARSMC) is designed for an advanced boiling water reactor (ABWR) nuclear power plant, to control reactor pressure, reactor water level and turbine power. The FARSMC is intended to replace the existing conventional controllers for the power range of 70% to 100% rated power. The controller has a recursive form that treats model uncertainty and external disturbances in an implicit way. Thus there is no need to specify uncertainties and disturbances for this controller design in advance. Moreover, the chattering problem common among conventional sliding-mode controllers is completely removed by this recursive sliding-mode control (RSMC) algorithm. The performance of the resulting RSMC is further improved by parameter adaptation using fuzzy logic algorithm, resulting in fuzzy-adapted RSMC (FARSMC). To apply RSMC technique, the original nonlinear plant model is first transformed to a canonical form. Simulations of the simplified ABWR model with the designed FARSMC indicate that FARSMC may result in better performance than the existing PI controllers in that the plant transient responses to the desired output step change have shorter settling time and smaller magnitude overshoot/undershoot. The control actions of the FARSMC are milder than those from the PI controllers. Robustness of the FARSMC with respect to power level variation and capability to reject external disturbances is also achieved. Successful fuzzy adapted sliding-mode controller design and implementation on the model shows that FARSMC may be a practical choice for nuclear power plant control.**

***Index Terms*—Adaptive control, fuzzy logic, nuclear power generation control, sliding-mode control.**

ACRONYMS

ABWR	Advanced boiling water reactor.
CVC	Control valve opening control.
FARSMC	Fuzzy-adapted recursive sliding-mode control, or fuzzy-adapted recursive sliding-mode controllers, depending on the context.
FWC	Feedwater flow control.
MIMO	Multi-input multi-output.
PI	Proportional-integral.
PIC	Proportional-integral control, or proportional-integral controllers, depending on the context.
RFC	Recirculation flow control.
RSMC	Recursive sliding-mode control.
SMC	Sliding-mode control.

Manuscript received July 1, 2003; revised November 2, 2003.

Z. Huang is with Thermoflow, Inc., Sudbury, MA 01776 USA (e-mail: hzy001@yahoo.com).

R. M. Edwards and K. Y. Lee are with Pennsylvania State University, University Park, PA 16802-1408 USA (e-mail: rmenuc@engr.psu.edu; kwanglee@psu.edu).

Digital Object Identifier 10.1109/TNS.2004.825100

NOMENCLATURE

Listed below are the variables in the ABWR plant model described in Section III. Control related variables can be found in the related context.

$A_{\rm cv}$	Throttle valve opening.
$A_{\rm iv}$	Intercept valve opening.
C_D	Doppler reactivity feedback coefficient.
$C_{\rm ip}$	Intermediate-pressure turbine inlet pressure change rate coefficient.
c_{ri}	Normalized precursor density.
C_V	Void reactivity feedback coefficient.
C_x	Correlation constant.
$C_{\Delta P}$	Steam pressure loss coefficient.
f_d	Fraction of heat generation from fission product decay.
f_f	Fraction of heat generation from fuel rod.
$f_{\rm hp}$	Mechanical power contribution factor of high-pressure turbine.
$f_{\rm ip}$	Mechanical power contribution factor of intermediate-pressure turbine.
h_f	Saturated liquid enthalpy.
$h_{\rm fw}$	Feedwater enthalpy.
h_g	Saturated steam enthalpy.
k	Effective neutron multiplication factor.
L	Reactor core water level deviation from setpoint.
L_1	Level change due to unbalance between feedwater flow and steam flow.
L_2	Level change due to change in core region void fraction.
L_3	Level change due to change in core exit plenum void fractions.
L_4	Level change due to deviation of steam flow from the steam driers.
$m_{\rm fw}$	Feedwater mass flow.
$\tilde{m}_{\rm fw}$	Intermediate variable related to feedwater transfer delay.
m_g	Core steam mass flow.
$m_{\rm hp}$	Steam flow to high-pressure turbine.
$m_{\rm ip}$	Steam flow to intermediate-pressure turbine.
m_r	Recirculation flow.
m_s	Steam flow.
n_o	Rated steady state neutron density (n/cm^3).
n_r	Normalized neutron density.
$P_{\rm ip}$	Pressure at intermediate-pressure turbine inlet.
P_t	Turbine throttle pressure.

P_v	Normalized reactor pressure.
Q_t	Total heat generation rate.
Q_f	Heat generation rate from fuel rod.
Q_g	Heat generation rate from fission.
Q_d	Decay heat rate.
u	Internal energy.
W_t	Turbine power output.
x	Normalized load demand.
x_e	Core exit steam quality.
x_{eR}	Rated core exit steam quality.
$\Delta h_{\rm sc}$	Core inlet subcooling.
ΔP	Pressure drop across main steam line.
α	Core steam void fraction.
Λ	Effective prompt neutron lifetime (s).
β	Fraction of delayed fission neutrons, $\beta = \sum_{i=1}^{2} \beta_i$.
β_i	Fraction of the ith group delayed neutrons.
$\delta\alpha$	Void fraction deviation from rated value at 100% power.
$\delta\Delta h_{\rm sc}$	Core inlet subcooling deviation.
δQ_f	Fuel rod heat flux deviation from rated value at 100% power.
$\delta\rho$	Reactivity (\$).
δx_e	Core exit steam quality deviation.
λ	Precursor decay constant ($\rm s^{-1}$).
τ_c	Reactor core mass transfer constant.
τ_d	Time constant of decay heat dynamics.
τ_f	Time constant of fuel rod heat transfer dynamics.
$\tau_{\rm dcR}$	Rated downcomer constant.
$\tau_{\rm fw}$	Feedwater time constant.
$\tau_{\rm hp}$	Time constant of steam transportation.
τ_V	Reactor pressure time constant.

I. Introduction

CONTROL of a nuclear power plant, or for that matter any complicated power plant, is challenging because: 1) the control is a multi-objective task for which many manipulated variables are coordinated to achieve satisfactory plant transients; 2) the system is nonlinear; and 3) many parameters are time-varying and the dynamic characteristics of the plant change with operating conditions. To design controllers, the plant dynamic model is usually simplified. Therefore discrepancies between the actual plant and the mathematical model are inevitable. This mismatch may come from unmodeled dynamics, variation in system parameters and/or the approximation of complex behavior by a straightforward model. In order to ensure that the resulting controller is capable of producing satisfactory results in this unfavorable situation, a robust controller is crucial to achieve reliable and safe automation of nuclear power plants. Linear robust control has become a well-established and mathematically rigorous control technique [1] and it has been comprehensively studied for integrated power control of an advanced boiling water reactor (ABWR) nuclear power plant [2]. However, it requires detailed uncertainties information, whose acquisition is somehow subjective and is a tedious process. Conservative estimation of uncertainties may result in no feasible controller design whereas underestimation leads to undesirable performance of the closed-loop system. In addition, linearization of the original nonlinear model is necessary and introduces another type of uncertainties. Because combination of all uncertainties is typically considered during the design of a linear robust controller, the resulting controller is usually unnecessarily conservative.

Sliding-mode control (SMC) technique belongs to the robust controller category, which deals with model uncertainties of simplified models. These uncertainties may come from unmodeled dynamics, variations in system parameters, or approximations of complex plant behaviors. An SMC controller is a particular type of varying structure system [3] featuring prescribed behavior of the closed loop system and robustness to parameter variations and external disturbances. SMC is a powerful approach to solve system state tracking problems. The architecture of SMC is simple and its design is directly oriented toward nonlinear systems—no linearization is needed. Like the linear robust control system, design of conventional SMC also needs plant uncertainties and external disturbance information. A typical intrinsic problem in implementing an SMC is "chattering", i.e., the control action changes with a very high frequency around a certain value when the controlled variable is close to the desired trajectory. By introducing recursive form, the resulting recursive SMC (RSMC) ([3], [4]) not only solves the intrinsic chattering problem of a conventional SMC but also features no need to describe uncertainties and disturbances in advance in some situations.

Generally speaking, the closed-loop system with SMC behaves like a linear system. Sometimes, however, nonlinear behavior is desirable for better performance. To this end, the nonlinear mapping characteristics of fuzzy systems [5] can play an important role. Some researchers have succeeded in merging fuzzy adaptation techniques into SMC design and the performance of the resulting systems is significantly improved [7].

Although sliding-mode control and fuzzy logic control techniques have been widely used in other fields [8], in nuclear industry, however, applications of these techniques seem to be much sparse and the studies of this topic are sporadic [9]. Shtessel applied SMC in space nuclear reactor system control and obtained good simulation results [9]. In that study, the improvement of the space reactor power system was reported for the reactor startup regime by applying SMC. Robustness and high accuracy in tracking of the reference thermal power profile were achieved. Huang and Edwards successfully applied RSMC to control ABWR turbine throttle pressure through manipulating turbine control valve opening [11]—simulation results show that the RSMC is superior to the existing PI controllers in that the RSMC results in milder control action and much less power surge than the PI controller; the response time for pressure setpoint change is much shorter with control of the RSMC.

In this paper, a robust multi-input multi-output (MIMO) controller based on fuzzy-adapted recursive sliding mode control (FARSMC) technique is designed for an ABWR plant overall control, specifically, to control: 1) turbine power; 2) reactor water level; and 3) turbine throttle pressure simultaneously to make them follow a demand or maintain a setpoint, through manipulation of reactor recirculation flow control (RFC), feedwater flow control (FWC), and turbine control valve opening control (CVC), respectively.

The remaining presentation is organized into five additional sections. In Section II a brief description of FARSMC algorithm is introduced, based on the concepts of recursive sliding-mode control and adaptation of sliding-mode control parameters. The ABWR model, of the original nonlinear form and of the derived input-output linearized form, is described in Section III. In Section IV, the FARSMC design features are described. Simulation results of the ABWR plant with the designed FARSMC and discussions are presented in Section V. Summary and conclusions are arranged in the last section—Section VI.

II. Fuzzy-Adapted Recursive Sliding-Mode Control

A. Recursive Sliding-Mode Control (RSMC) for an MIMO System

Consider a nonlinear MIMO square system[1] of the form

$$y_i^{(n_i)} = f_i(\mathbf{x}) + \sum_{j=1}^{m} g_{ij}(\mathbf{x})(u_j + d_j) \quad i = 1, \ldots, m; \quad j = 1, \ldots, m \tag{1}$$

or in a compact form

$$\mathbf{y}^{(n)} = \mathbf{f}(\mathbf{x}) + \mathbf{G}(\mathbf{x})(\mathbf{u} + \mathbf{d}) \tag{2}$$

where

$$\mathbf{y}^{(n)} = \left(y_1^{(n_1)}, y_2^{(n_2)}, \ldots, y_m^{(n_m)}\right)^T \tag{3}$$

$$\mathbf{f} = (f_1, f_2, \ldots, f_m)^T \tag{4}$$

$$\mathbf{G} = \begin{pmatrix} g_{11} & \cdots & g_{1m} \\ \vdots & \ddots & \vdots \\ g_{m1} & \cdots & g_{mm} \end{pmatrix}. \tag{5}$$

$\mathbf{u} = (u_1, u_2, \ldots, u_m)^T$ is the control input vector, $\mathbf{d} = (d_1, d_2, \ldots, d_m)^T$ is the disturbance vector, and the state $\mathbf{x}$ is composed of y_i's and their first $(n_i - 1)$ derivatives.

The nonlinear dynamics of $\mathbf{f}(\mathbf{x})$ and matrix $\mathbf{G}(\mathbf{x})$ are not exactly known but they are estimated by their nominal forms of $\hat{\mathbf{f}}$ and $\hat{\mathbf{G}}$, respectively. The uncertainties in $\mathbf{f}$ are expressed in additive form of their individual elements, as in the following:

$$|f_i - \hat{f}_i| \le F_i \quad i = 1, \ldots, m \tag{6}$$

where F_i's are upper bounds of uncertainties in $f_i(\mathbf{x})$'s, and the uncertainties in $\hat{\mathbf{G}}$ is expressed in a multiplicative form as in the following:

$$\mathbf{G} = (\mathbf{I} + \Delta)\hat{\mathbf{G}}, \quad |\Delta_{ij}| \le D_{ij}, \quad i = 1, \ldots, m; \quad j = 1, \ldots, m \tag{7}$$

where $\mathbf{I}$ is the $m \times m$ identity matrix and Δ is the error matrix defined by Δ_{ij}.

In order to facilitate controller design and analysis, the system is assumed to meet the matching condition, i.e., with uncertainties in the components $g_{ij}(i, j = 1, 2, \ldots, m)$ considered, the matrix $\mathbf{G}$ is invertible. This assumption assures the controllability of the system.

For the state-tracking problem, the goal of controller design is to find control $\mathbf{u}$ such that the plant outputs track the desired trajectory $\mathbf{y}_d$, in the presence of uncertainties and perturbations.

Let $e_i(t) = y_i(t) - y_{di}(t)$ be the tracking error in the output $y_i(t)$ and specify a switching vector containing individual switching functions

$$\mathbf{s} = (s_1, s_2, \ldots, s_m)^T \tag{8}$$

$$s_i = \left(\frac{d}{dt} + \gamma_{i(n_i-1)}\right) \cdots \left(\frac{d}{dt} + \gamma_{i2}\right)\left(\frac{d}{dt} + \gamma_{i1}\right) e_i \quad i = 1, 2, \ldots, m \tag{9}$$

where $\gamma_{ij}, i = 1, 2, \ldots, m; j = 1, 2, \ldots, n_i - 1$ are strictly positive constants, and are called "control bandwidth" in some literatures.

Expression (9) can be rewritten into two forms.

One is in polynomial-like form, which is more convenient to derive the control algorithm

$$s_i = \sum_{j=0}^{n_i-1} c_{ij}\left(y_i^{(j)} - y_{di}^{(j)}\right) \tag{10}$$

where $c_{i,n_i-1} = 1$, and the roots of the polynomial $[1\, c_{i,n_i-2}\, c_{i,n_i-3} \ldots c_{i,1}\, c_{i,0}]$ are equal to $[\gamma_1\, \gamma_2 \ldots \gamma_{n_i-1}]$. The other is the recursive form, which is more meaningful and will be used to tune the designed sliding-mode controller

$$\begin{aligned} s_i &= s_{i,n_i-1} = \dot{s}_{i,n_i-2} + \gamma_{i,n_i-1} s_{i,n_i-2} \\ &\vdots \\ s_{i,2} &= \dot{s}_{i,1} + \gamma_{i,2} s_{i,1} \\ s_{i,1} &= \dot{e}_i + \gamma_{i,1} e_i. \end{aligned} \tag{11}$$

Now specify a Lyapunov function as a quadratic form of the switching function $\mathbf{s}$

$$v = \mathbf{s}^T\mathbf{s}/2. \tag{12}$$

The goal of controller design is to find a control vector $\mathbf{u}$ such that the following reaching condition is met in the presence of uncertainties and disturbances

$$\dot{v} = -\mathbf{s}^T\mathbf{\Gamma}\mathbf{s} \tag{13}$$

where $\mathbf{\Gamma}$ is a positive definite constant matrix. Compared with the frequently used reaching condition $\dot{v} \le -\sum_{i=1}^{m} \eta_i |s_i|$, where $\eta_i > 0$, (13) specifies a "softer" reaching condition. This softer reaching condition is introduced to avoid the chattering problem and to dynamically adapt the system to the uncertainties and disturbances.

Combining (12) and (13) yields the following equality:

$$\dot{\mathbf{s}} + \mathbf{\Gamma}\mathbf{s} = 0 \tag{14}$$

which is the new reaching condition for the system.

Combined with (2) and (1), the time derivative of switching function $\mathbf{s}$ can be developed into the following form:

$$\dot{\mathbf{s}} = \hat{\mathbf{s}} + \mathbf{G}(\mathbf{u} + \mathbf{d}) \tag{15}$$

[1] A square system is a system that has the same number of inputs as that of outputs.

where

$$\hat{\mathbf{s}} = [\hat{s}_1\ \hat{s}_2\ \ldots\ \hat{s}_m]^T \tag{16}$$

$$\hat{s}_i = -y_{di}^{(n_i)} + \sum_{j=1}^{n_i-1} c_{i,j-1}\left(y_i^{(j)} - y_{di}^{(j)}\right) + f_i(\mathbf{x}). \tag{17}$$

In order for the sliding surfaces $\mathbf{s} = 0$ to be attractive, the control $\mathbf{u}$ can be derived by substituting (15) into (14), yielding

$$\mathbf{u} = \mathbf{u}_{\text{eq}} - \mathbf{G}^{-1}\boldsymbol{\Gamma}\mathbf{s} \tag{18}$$

where $\mathbf{u}_{\text{eq}}$ is the equivalent control

$$\mathbf{u}_{\text{eq}} = -\mathbf{G}^{-1}\hat{\mathbf{s}} - \mathbf{d}. \tag{19}$$

From (19), (16) and (17), it can be seen that the equivalent control is a function of $\mathbf{f}(\mathbf{x}), \mathbf{G}(\mathbf{x})$, which are usually hard to obtain and usually contain uncertainties and disturbance $\mathbf{d}$, which is usually unknown. These factors can be automatically taken into account by introducing a recursive form of control algorithm. Combining (15), (18), and (19), the recursive form is

$$\mathbf{u} = \mathbf{u} - \mathbf{G}^{-1}(\dot{\mathbf{s}} + \boldsymbol{\Gamma}\mathbf{s}). \tag{20}$$

In continuous-time domain, (20) is easy to implement by slightly changing the form to

$$\mathbf{u}(t) = \mathbf{u}(t - \delta t) - \mathbf{G}^{-1}(\dot{\mathbf{s}} + \boldsymbol{\Gamma}\mathbf{s}) \quad \delta t \to 0. \tag{21}$$

This form has the same format as the algorithm used in [4] although the nonlinear system for which the controller is designed in that paper is different from the one in this study.

It is shown in [4] that in continuous-time systems with no computational delay, the condition for the Lyapunov function v specified in (13) is satisfied after the renewed control value specified in (21) is implemented. Because $\boldsymbol{\Gamma}$ is positive definite, the time derivative of the Lyapunov function is negative definite, meaning that the sliding surface $\mathbf{s} = \mathbf{0}$ is attractive.

In the discrete-time domain, the control updating in (20) can be implemented by using the following form:

$$\mathbf{u}(t) = \mathbf{u}(t - T) - \mathbf{K}\mathbf{G}^{-1}(\dot{\mathbf{s}} + \boldsymbol{\Gamma}\mathbf{s}) \tag{22}$$

where T is the period for controller implementation and $\mathbf{K}$ is a diagonal matrix

$$K = \begin{pmatrix} K_1 & & 0 \\ & \ddots & \\ 0 & & K_m \end{pmatrix} \tag{23}$$

whose diagonal elements are subject to tuning during implementation.

If the constant matrix $\boldsymbol{\Gamma}$ in the reaching condition (13) takes the diagonal form, considering (11), the term $\dot{\mathbf{s}} + \boldsymbol{\Gamma}\mathbf{s}$ is simply an extension of sliding surfaces with one further step in the recursive form

$$\begin{aligned} s_{si} &= \dot{s}_i + \gamma_i s_i \\ \text{with} \\ s_i &= s_{i,n_i-1} = \dot{s}_{i,n_i-2} + \gamma_{i,n_i-1} s_{i,n_i-2} \\ &\vdots \\ s_{i,2} &= \dot{s}_{i,1} + \gamma_{i,2} s_{i,1} \\ s_{i,1} &= \dot{e}_i + \gamma_{i,1} e_i \end{aligned} \tag{24}$$

which defines a new switching vector $\mathbf{s}_s$. In this case, the control law (22) becomes

$$\mathbf{u}(t) = \mathbf{u}(t - T) - \mathbf{K}\mathbf{G}^{-1}\mathbf{s}_{\mathbf{s}}. \tag{25}$$

To smooth the control signal and to implement the controller in the continuous-time domain, (25) is replaced with the new control law

$$\dot{\mathbf{u}}(t) = -\hat{\mathbf{K}}\mathbf{G}^{-1}\mathbf{s}_{\mathbf{s}} \tag{26}$$

where $\hat{\mathbf{K}} = \mathbf{K}/T$ or

$$\mathbf{u}(t) = -\int \hat{\mathbf{K}} G^{-1}\mathbf{s}_{\mathbf{s}}\, dt. \tag{27}$$

B. Fuzzy Adaptation of RSMC Parameters

One of the distinguishing features of the SMC is that the closed-loop system behaves like a linear system once the system state is on the sliding surface. The tracking error, if it's not zero initially, will converge to zero exponentially along the sliding surface. The system behavior can be predetermined by setting the sliding-mode parameters. The selection of constant sliding-mode variables is restricted by the following dilemma: large values of γ_{ij}'s will cause fast system response but may excite the unmodeled high frequency dynamics, leading to instability of the closed system; on the other hand, if γ_{ij}'s are too small, the system responds too slowly. In this sense, nonlinear system behavior is desirable. Consider a second order single-input single-output system for example, where the switching function is typically defined as: $s = \dot{e} + \gamma e$, and the sliding line on the phase-portrait and the time response with the initial condition $e = 1$ are shown in Fig. 1. For comparison, the phase portrait and the time response of a nonlinear sliding surface are also shown in the figure. It is clear from comparison that the settling time of the system with nonlinear sliding surface is greatly reduced.

Based on the above observation, it is desirable to design the sliding-mode controller with the predetermined system behavior defined as a nonlinear system, specifically, the bandwidth of the sliding-mode controller may vary with the system status in order to achieve better performance. This concept was realized in the study by Temeltas [12]. In that study, two fuzzy approximators were employed, one adjusted the slope of the sliding surface slope and the other adjusted the approaching rate in the reaching phase (the term "reaching phase" is illustrated in Fig. 2). The resulting fuzzy adapted sliding-mode controller led to more robust tracking of the system.

In this study, triangular membership functions are used for all fuzzy values, as shown in Fig. 3. From this figure, it is clear that the membership function information related to a fuzzy variable can be completely represented with three components: 1) variable name; 2) term set, which is the set of linguistic labels of all fuzzy sets of a fuzzy variable; and 3) peak value set, which is the set of the peak values corresponding to the linguistic labels in the term set. These three components are $x, \{A^1, A^2, A^3, A^4, A^5, A^6, A^7\}$ and $\{\bar{x}_{i,1}, \bar{x}_{i,2}, \bar{x}_{i,3}, \bar{x}_{i,4}, \bar{x}_{i,5}, \bar{x}_{i,6}, \bar{x}_{i,7}\}$ in Fig. 3, respectively.

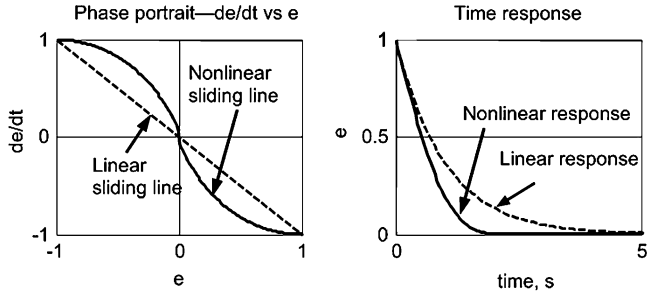

Left: phase portrait; Right: time response with initial value of 1
Dashed line: linear switching function; Solid line: nonlinear switch function.

Fig. 1. Comparison of system behavior with linear and nonlinear sliding surfaces.

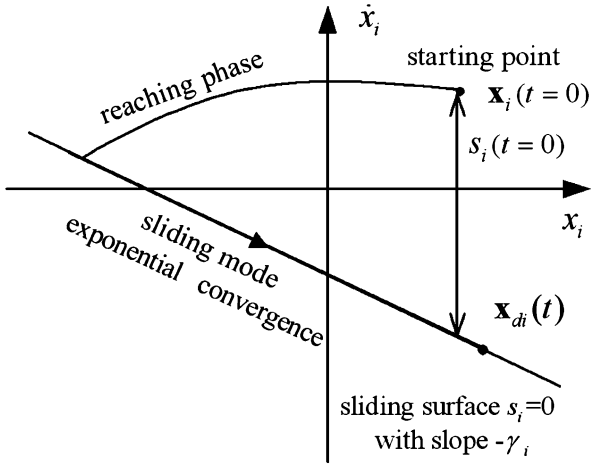

Fig. 2. Graphical illustration of sliding surface and sliding condition.

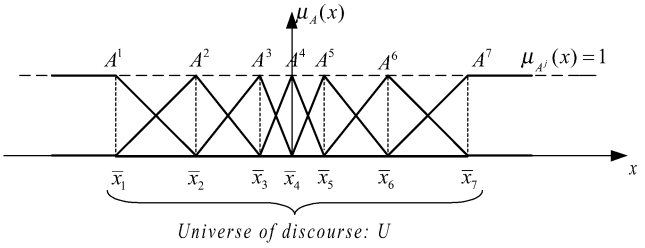

c) Triangular membership functions a fuzzy variable
A^j's are linguistic labels of fuzzy sets and $\bar{x}_j$'s are corresponding peak values at which the membership functions are 1.

Fig. 3. Illustration of fuzzy logic membership functions.

III. ABWR Model Description

To demonstrate the feasibility of FARSMC application in nuclear power plant control, a simplified ABWR power range model is used. The model calculates the neutronic, thermal-hydraulic, and turbine responses in conjunction with power control systems. This model is the same as that used to design a linear robust controller by Shyu and Edwards [2] and to design a group of fuzzy logic controllers by Huang, Lee and Edwards. [13] All parameters in the model are normalized to rated conditions on a per unit basis.

In conjunction with the plant model, the original simulation model also contains the PI control system designed by the vendor, which will be used for controller performance comparison in this study. The original control system consists of three main subsystems: reactor power control, reactor water level regulation, and pressure regulation. For a boiling water reactor, power control is implemented through reactor recirculation flow adjustment or control rod movement. In the 70%–100% rated power range, which is of the interest in this study, the reactor is controlled only by recirculation flow adjustment on the basis of load demand error. The reactor water level control is controlled by adjusting feedwater flow rate, and the pressure control is implemented by adjusting the turbine throttle valve opening.

Detailed model description can be found in [2] and [14]. The equations directly related to the derivation of the forthcoming canonical-form dynamic equations are as follows.

A. Neutron Dynamics and Heat Generation Model[2]

The neutron dynamics is represented by the point kinetics with two delayed neutron groups

$$\dot{n}_r(t) = \frac{\delta\rho(t)-\beta}{\Lambda} n_r(t) + \sum_{i=1}^{2} \frac{\beta_i}{\Lambda} c_{ri}(t) \tag{28}$$

$$\dot{c}_{ri}(t) = \lambda_i n_r(t) - \lambda_i c_{ri}(t), \quad i = 1 \ldots 2 \tag{29}$$

where n_r is neutron density, representing reactor power.

Heat generation Q_t in the reactor is calculated from the following:

$$Q_t = Q_f + (1-f_f)[(1-f_d)n_r + Q_d] \tag{30}$$

where Q_f and Q_d are the heat generation from fuel rods and decay heat rate, respectively, whose dynamics are defined as

$$\dot{Q}_f = (f_f Q_g - Q_f)/\tau_f \tag{31}$$

and

$$\dot{Q}_d = (f_d n_r - Q_d)/\tau_d. \tag{32}$$

B. Thermal Hydraulic Model

The thermal hydraulic model is developed, from mass and energy conservation equations, to calculate the reactor vessel pressure (P_V), void fraction (α) and reactor water level (L)

$$\dot{P}_V = \left\{ Q_t + m_{\rm fw}\frac{h_{\rm fw}-u}{(h_g-h_{\rm fw})_R} - m_s\frac{h_g-u}{(h_g-h_{\rm fw})_R} \right\} / \tau_V \tag{33}$$

$$m_g = \frac{(h_g-h_{\rm fw})_R}{(h_g-h_f)} \left[Q_t - m_{\rm fw}\frac{h_f-h_{\rm fw}}{(h_g-h_{\rm fw})_R} - \tau_C \dot{P}_V \right] \tag{34}$$

$$\tau_{\rm dcR}\Delta\dot{h}_{\rm sc} = m_{\rm fw}[1 + C_h(1-\tilde{m}_{\rm fw})] - m_r\Delta h_{\rm sc} \tag{35}$$

$$\dot{\tilde{m}}_{\rm fw} = (m_{\rm fw} - \tilde{m}_{\rm fw})/\tau_{\rm fw} \tag{36}$$

$$\delta\alpha = a_\alpha(\delta x_e) + b_\alpha(\delta\Delta h_{\rm sc}) + c_\alpha(\delta x_e)(\delta\Delta h_{\rm sc}) \tag{37}$$

$$L = L_1 + L_2 + L_3 + L_4 \tag{38}$$

where L_1 reflects the contribution of the mismatch between feedwater flow and steam flow to the reactor water deviation

$$\dot{L}_1 = a_L(m_{\rm fw} - m_s) \tag{39}$$

and $L_2 - L_4$ are related to reactor void fraction change and steam mass flow dynamics, etc.

[2]In this section, only some important variables are explained following the equation where they first appear. See the nomenclature table for descriptions of other variables.

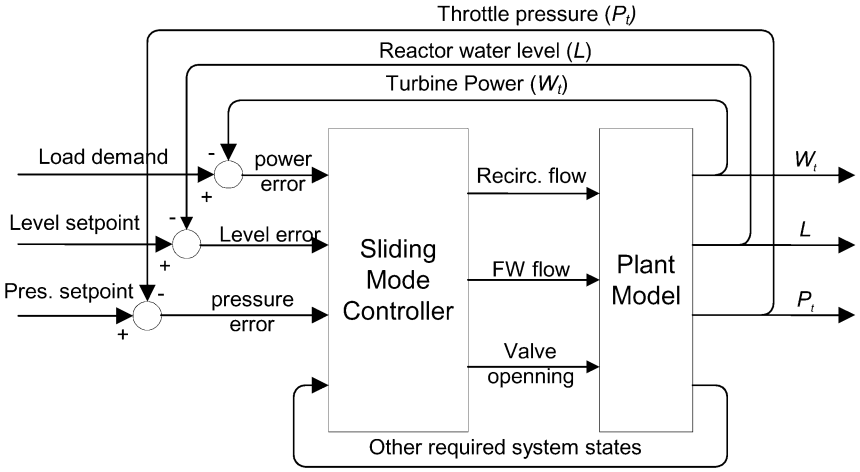

Fig. 4. Connection of sliding-mode controller for the ABWR system.

C. Turbine Model

Turbine throttle pressure (P_t) is related to the reactor pressure by the relation

$$P_t = P_v - C_{\Delta P} m_s^2. \tag{40}$$

During normal operation, turbine bypass valve is not involved, thus, the steam flow can be expressed as

$$m_s = P_t A_{\rm cv} \tag{41}$$

where $A_{\rm cv}$ is the turbine throttle valve opening.

The ABWR plant operation requires that the turbine pressure (P_t) setpoint change with load demand according to the following relations:

$$P_t = 1 + (x - x^2)/12 \tag{42}$$

where x is the normalized load demand.

The high-pressure (HP) and intermediate-pressure (IP) turbines contribute to the turbine power (W_t)

$$W_t = f_{\rm hp} m_{\rm hp} + f_{\rm ip} m_{\rm ip} \tag{43}$$

where $m_{\rm hp}$ and $m_{\rm ip}$ are steam flow to HP and IP turbines, respectively, obtained from the following dynamics:

$$\begin{aligned} \dot{m}_{\rm hp} &= (m_s - m_{\rm hp})/\tau_{\rm hp} \\ \dot{P}_{\rm ip} &= C_{\rm ip}(m_{\rm hp} - m_{\rm ip}) \\ m_{\rm ip} &= P_{\rm ip} A_{\rm iv}. \end{aligned} \tag{44}$$

IV. FARSMC Design for an ABWR Plant

The FARSMC designed in this study is based on a nonlinear system, which is externally deemed as a 3-input 3-output MIMO system: three input signals—reactor recirculation flow (m_r), feedwater flow $(m_{\rm fw})$ and turbine throttle valve opening $(A_{\rm cv})$—are used to control the corresponding three outputs—turbine power (W_t), reactor water level deviation (L) and turbine throttle pressure (P_t), respectively. These three outputs are fed back to form corresponding output errors that are used to generate the switch functions for sliding-mode controller design. Some other plant states, such as the reactor vessel pressure, steam flow, delayed neutron precursor density, etc., are also fed back to serve as controller inputs. The overall structure of the ABWR system with the controller connection is depicted in Fig. 4. Design objectives of FARSMC are defined as: under all situations where power is above 70% of rated power, the plant should be able to track load demand, pressure setpoint, and reactor water level setpoint to an acceptable degree so that the plant performs satisfactorily and the reactor safety will not be jeopardized, within an acceptable time period and with an acceptable amount of steady state error.

The nonlinear model presented in Section III cannot be directly used for SMC design because the model is not presented in the required canonical form as in (1). To apply FARSMC for ABWR plant overall control, each input must appear explicitly in the final differential equation of its corresponding output, i.e., the highest order derivatives of W_t, L and P_t must contain $m_r, m_{\rm fw}$ and $A_{\rm cv}$, respectively, as one of their corresponding inputs. The model conversion is first presented in Section IV-A. Based on the model in the new form, the FARSMC controller design is then described Section IV-B and IV-C.

A. Input–Output Linearization

In order to obtain the required dynamic model in the canonical-form and to limit the relative order of the resulting model to a reasonable number suitable for controller design, some approximations are first made.

1) Approximations: Heat generation involves the neutron dynamics. First, it is simplified with a one-delayed neutron group model

$$\dot{n}_r(t) = \frac{\delta\rho(t) - \beta}{\Lambda} n_r(t) + \frac{\beta}{\Lambda} c_r(t) \tag{45}$$

$$\dot{c}_r(t) = \lambda n_r(t) - \lambda c_r(t) \tag{46}$$

with

$$\lambda = \frac{\beta_1 + \beta_2}{\beta_1/\lambda_1 + \beta_2/\lambda_2}. \tag{47}$$

The prompt-jump approximation for neutron density n_r can be derived from (45)

$$n_r(t) = \frac{c_r(t)}{1 - \Delta K} \tag{48}$$

where $\Delta K = \delta\rho(t)/\beta$ is the net reactivity change in the unit of dollar. Due to the small magnitude of ΔK occurred in most transients, (48) is further approximated as

$$n_r(t) = (1 + \Delta K)c_r(t) \tag{49}$$

which can further be approximated as

$$n_r = [1 + C_D(Q_t - 1) + C_V(b_\alpha \delta\Delta h_{\rm sc} - a_\alpha x_{eR})]c_r + C_V a_\alpha x_{eR}[1 - C_x(1 - m_g)]m_g c_r m_{ri}. \tag{50}$$

The heat transfer process described in (30)–(32) can be approximated as

$$\dot{Q}_t = (n_r - Q_t)/\tau_f. \tag{51}$$

Based on the approximations described above, the heat generation dynamics is approximated as

$$\tau_f \dot{Q}_t = [1 + C_D(Q_t - 1) + C_V(b_\alpha \delta\Delta h_{\rm sc} - a_\alpha x_{eR})]c_r - Q_t + C_V a_\alpha x_{eR}[1 - C_x(1 - m_g)]m_g c_r m_{ri}. \tag{52}$$

The turbine inlet pressure can be approximated from the implicit equations (40)–(41) to the explicit form [14]

$$P_t = P_v - C_{\Delta P} A_{\rm cv}^2 P_v^2. \tag{53}$$

The input-output relationship of the ABWR system in a compact canonical form can be obtained from (43), (38), and (53) with a series of time derivatives and substitutions

$$\begin{bmatrix} \dddot{W}_t \\ \ddot{L} \\ \ddot{P}_t \end{bmatrix} = \begin{bmatrix} f_W(\mathbf{x}) \\ f_L(\mathbf{x}) \\ f_P(\mathbf{x}) \end{bmatrix} + \mathbf{G} \begin{bmatrix} m_{ri} \\ \dot{m}_{\rm fw} \\ \ddot{A}_{\rm cv} \end{bmatrix} \tag{54}$$

where $f_W(\mathbf{x}), f_L(\mathbf{x})$ and $f_P(\mathbf{x})$ are the functions of the three inputs and other plant states, whose expressions can be found in [14]; m_{ri} is the new input from $m_r, m_{ri} = 1/m_r$, and $\mathbf{G}$ is a 3×3 gain matrix

$$\mathbf{G} = \begin{bmatrix} g_{11} & g_{12} & g_{13} \\ g_{21} & g_{22} & g_{23} \\ g_{31} & g_{32} & g_{33} \end{bmatrix} \tag{55}$$

whose elements g_{ij}'s are also functions of the system inputs and other plant states.

2) Internal Stability Analysis: The relative degree of the above system is [3,2,2] and the total relative degree is $r = 7$. The order of the original ABWR model is 11 in the operating region of 70%–100% rated power. There are four hidden states. For sliding-mode controller design, it is necessary to identify these states and verify the internal stability of the system.

The formal procedure to verify the internal stability is to analyze the zero dynamics of the subsystem to represent the dynamics of the internal states, which is generally very complicated. In this study, the internal states are identified as

- the precursor density c_{r1} and c_{r2};
- the reactor coolant inlet subcooling $\Delta h_{\rm sc}$;
- one state related to the reactor heat generation model order reduction.

Stability of c_{r1} and c_{r2} are straight forward: the transfer function from n_r to c_{ri}'s can be obtained from (29) as: $c_{ri}(s)/n_r(s) = \lambda_i/(\lambda_i + s)$, whose eigenvalues are strictly negative $(-\lambda_i)$, which leads to the bounded-input bounded-output characteristics of this subsystem. Thus, the internal dynamics of c_{ri}'s is verified. Similarly, the stability of Q_f and Q_d can be verified from (31) and (32). Therefore, the missing state due to model order reduction is also stable. Finally, the stability of $\Delta h_{\rm sc}$ can be verified by analyzing (35) and (36) after linearization of these equations at an initial state.

The stability of the other seven states is guaranteed if the sliding-mode controller is successfully designed, which is the topic of Section IV-B, for the nonlinear system described by (54). These variables are nonlinear transformations of the states in the new nonlinear system—time derivatives of W_t, L and P_t of various orders, whose stability are achieved by the sliding-mode controller design.

B. Recursive Sliding-Mode Controller (RSMC) Design

According to the control algorithm specified in (27) and the ABWR canonical form dynamics in (54), the SMC control law for ABWR system is rewritten into the following form:

$$\mathbf{u}(t) = \int \mathbf{K}\mathbf{G}^{-1}\mathbf{s}\, dt \tag{56}$$

where control vector $\mathbf{u} = [m_{ri}\, \dot{m}_{\rm fw}\, A_{cv}]^T$, the control gain $\mathbf{K}$ is redefined as

$$\mathbf{K} = \begin{bmatrix} K_W & & \mathbf{0} \\ & K_L & \\ \mathbf{0} & & K_P \end{bmatrix} \tag{57}$$

and the vector $\mathbf{s}$ of sliding function is redefined as

$$\begin{aligned} \mathbf{s} &= [s_1\, s_2\, s_3]^T \\ s_i &= s_{i,n_i} \quad i = 1, 2, 3 \\ s_{i,j} &= \dot{s}_{i,j-1} + \gamma_{i,j} s_{i,j-1} \quad j = 1, 2, \ldots, n_i \\ s_{i,0} &= e_i \end{aligned} \tag{58}$$

and s_1, s_2 and s_3 are the newly defined switching functions corresponding to turbine power, reactor water level, and throttle pressure, respectively, and $n_1 = 3, n_2 = 2$, and $n_3 = 2$.

The remaining task is to determine the sliding-mode controller parameters and to refine the controller. However, special treatment is necessary before directly applying the control algorithm. First, the canonical-form system dynamics equations are derived with some simplifications. Second, the system state information is needed to calculate the matrix $\mathbf{G}$ in (54) and the controller design in this study takes the practical application situation into account.

1) Decoupling Matrix Simplification: The approximation made during the input/output (I/O) linearization changes the dynamic behavior of the system, especially for the high-order derivatives of the related variable. For example, the relative degree is 3 for the turbine power; therefore the sliding-mode control is based on the assumption that the change of input (recirculation flow) should be immediately reflected in the third-order time derivative of the turbine power. However, the actual relative order of turbine power is greater than 3 due to the delayed neutron dynamics, thus there is a time delay in the change of the third-order derivative in response to the control signal input.

To eliminate the adverse effects of the incorrect coupling information provided by the I/O linearization, the off-diagonal el-

ements of the decoupling matrix $\mathbf{G}$ are set to zero, i.e., the coupling effects of the control inputs are not considered explicitly, rather, they are handled with the high-order derivative information of the outputs. This treatment is also performed in [3], resulting in a simpler design whereas the controller performance is not obviously degraded.

2) System State Acquisition: The control algorithm for this study is specified in (27), where the decoupling matrix $\mathbf{G}$ needs the following variables to be evaluated: throttle valve opening $A_{\rm cv}$, reactor core steam mass flow m_g, delayed neutron precursor density c_r, steam mass flow out of the reactor vessel m_s, and reactor vessel pressure P_v. Of these variables, $A_{\rm cv}, m_s$ and P_v are available from control or measurement; but c_r and m_g are system internal states that need to be estimated.

Delayed neutron precursor density $c_r(t)$ is estimated from neutron density $n_r(t)$ with a first order filter described by (46).

The steam mass flow m_g does not agree well with the steam flow out of the reactor vessel (m_s). In order to obtain a better signal for m_g, a filter is designed according to (34)

$$m_g = a_{mg}Q_t + b_{mg}m_{\rm fw} + c_{mg}m_s \tag{59}$$

where Q_t is obtained from a transfer function

$$\frac{Q_t(s)}{n_r(s)} = \frac{[\tau_d(1-f_d)s+1][\tau_f(1-f_f)s+1]}{(\tau_d s+1)(\tau_f s+1)}. \tag{60}$$

To obtain switching functions defined in (58), the following approximations are used:

$$\dot{s}_{i,j}(t) = (s_{i,j-1}(t) - s_{i,j-1}(t-T))/T$$

with

$$i = 1, 2, \ldots, m; j = 1, 2, \ldots, n_i - 1$$

and

$$s_{i,0} = e_i \tag{61}$$

where T is the sampling period and $T = 0.5$ second in this study.

3) Controller Design and Parameter Selection: With the off-diagonal elements set to zero and the gain matrix $\mathbf{K}$ defined in (23), the RSMC controller design becomes the design of three controllers for the decoupled subsystems.

Tuning of the RSMC parameters, control bandwidths γ_{ij}'s and control gains K_i's, may be done in practice experimentally. However, there are some limitations on the determination of γ_{ij}. Three factors limiting the choice of γ_{ij} are listed in [15]: 1) system resonant modes; 2) neglected time delays; and 3) sampling rate, and the limit for γ_{ij} is

$$\gamma \le \gamma_{\max} = \min\left(\frac{2}{3}\pi v_R, \frac{1}{3}T_d, \frac{1}{5}T_s\right) \tag{62}$$

where v_R is the lowest unmodeled system resonant frequency, T_d is the unmodeled time-delay, and T_s is the sampling time. The parameters used in the final controller design are listed in Table I.

C. Fuzzy Adaptation of RSMC Parameters

Application of RSMC to the ABWR nonlinear model [14] indicates a slower response of the RSMC compared with the existing PI controllers. Shown in Fig. 5 is an illustration of the slow reactor water level response under the control of RSMC with the controller parameter selected so that the system response is as fast as possible while the system remains stable. This phenomenon is expected because of the long-tail feature of the zero-approaching property of the sliding-mode controllers. This problem can be solved by the introduction of a fuzzy parameter-adaptation scheme.

TABLE I
LIST OF SLIDING-MODE CONTROLLER PARAMETERS.

i*	K_i**	γ_{i1}	γ_{i2}	γ_{i3}
1	0.2	0.1	0.5	1
2	0.3	0.05	0.1	
3	6	0.1	0.4	

Note:
* i=1: Recirculation Flow Controller (RFC);
i=2: Feedwater Flow Controller (FWC);
i=3: Pressure Regulator (PR)
** K_1, K_2 and K_3 correspond to $K_{\rm W}$, $K_{\rm L}$ and $K_{\rm P}$ in (57), respectively.

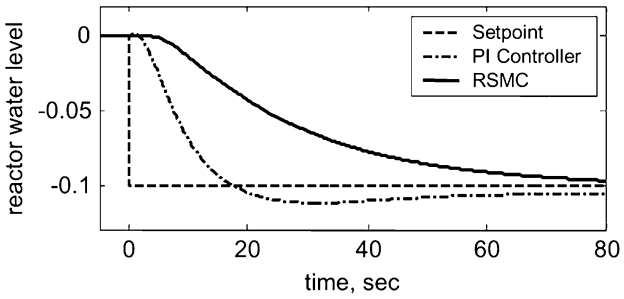

Fig. 5. Illustration of reactor water level slow response under control of RSMC.

Based on the observation in Section II-B, it is desirable to design the sliding-mode controller with the predetermined system behavior defined as a nonlinear system, specifically, the bandwidth of the sliding-mode controller may vary with the system status in order to achieve a better performance.

From Table I, it can be seen that for each of the sliding-mode control subsystems, the sliding surface parameters satisfy the following relationship: $\gamma_{ij} < \gamma_{i,j+1}$, thus the main factor to limit system performance is γ_{i1}. For simplicity, it suffices to adjust only the first parameter γ_{i1} for the purpose of settling time reduction for each controller.

In this work, fuzzy adaptation of γ_{i1} is performed by a fuzzy system with the absolute value of the tracking error e_i and the corresponding sliding parameter γ_{i1} as its input and output, respectively.

The fuzzy rules for γ_{i1} read as

$$Ru(j): \text{IF } |e_i| \text{ is } L_{ei}^j \text{ THEN } \gamma_{i1} \text{ is } L_{\gamma_{i1}}^j$$

where $i = 1, 2, 3$, represent recirculation flow control (RFC), feedwater flow control (FWC), and pressure regulation (PR), respectively and $j = 1, 2, \ldots, n_{fi}$, where n_{fi} is the number of fuzzy rules; and L_{ei}^j and $L_{\gamma_{i1}}^j$ are the linguistic labels of fuzzy sets in $|e_i|$ and γ_{i1}, respectively.

Triangular membership functions are used for all fuzzy values.

TABLE II
FUZZY RULE TABLE FOR SMC PARAMETER ADAPTATION

L_{ei}	ZE	VS	SM	MD	LG
$L_{\gamma i1}$	LG	ML	MD	MS	SM

TABLE III
MEMBERSHIP FUNCTIONS FOR SLIDING SURFACE SLOPE ADAPTATION

Part (a) RFC	L_{e_W}	ZE	VS	SM	MD	LG
	$\bar{e}_W$	0.001	0.003	0.01	0.03	0.1
	$L_{\gamma_{11}}$	LG	ML	MD	MS	SM
	$\bar{\gamma}_{11}$	0.80	0.68	0.42	0.23	0.10
Part (b) FWC	L_{e_L}	ZE	VS	SM	MD	LG
	$\bar{e}_P$	0.00	0.003	.01	0.03	0.10
	$L_{\gamma_{21}}$	LG	ML	MD	MS	SM
	$\bar{\gamma}_{21}$	0.20	0.19	0.18	0.15	0.10
Part (c) PR	L_{e_P}	ZE	VS	SM	MD	LG
	$\bar{e}_P$	0.0001	0.0003	0.0010	0.0030	0.01
	$L_{\gamma_{31}}$	LG	ML	MD	MS	SM
	$\bar{\gamma}_{31}$	0.50	0.30	0.20	0.15	0.10

Note: 1. Variables e_W, e_L and e_P are the alternative expressions for e_1, e_2 and e_3, mentioned above.
2. Upper bar represents the peak values for corresponding fuzzy values of a fuzzy variable.

The n_{fi}'s are set to 5 for all three controllers. The term set of L_{ei} and $L_{\gamma i}$ are specified as $[ZE\ VS\ SM\ MD\ LG]$ and $[LG\ ML\ MD\ MS\ SM]$, respectively, and the fuzzy rule bases are set to be of the same pattern, which is listed in Table II.

Membership functions of the fuzzy systems defining the nonlinear sliding surfaces, presented with the three components mentioned above, for turbine power control, reactor water level control and pressure regulation are listed in Parts a), b), and c) of Table III, respectively.

V. SIMULATION RESULTS AND DISCUSSIONS

The FARSMC designed in Section IV have been implemented on the original nonlinear ABWR simulation model discussed in Section III. In this section, simulation results are presented for some selected cases, including output tracking and disturbance rejection problems. Output tracking problems include: 1) load demand change; 2) reactor water level setpoint change; and 3) pressure setpoint change.

A. Load Demand Step Change

Shown in Fig. 6 are the responses of the selected variables to a step change of load demand from 90% to 100% rated power under control of the FARSMC and the existing PI controllers (PIC). Simulation results show that the introduction of the fuzzy parameter adaptation for the sliding-mode controller parameters has solved the extended settling-time problem as discussed in Section IV-C.

Comparison between the performances of the FARSMC and the conventional PI controllers are summarized as follows.

- The turbine power responses (plot a) with the two control methods are comparable, with about the same settling time and control action.
- As for pressure control, according to (42), there is a step change in turbine pressure setpoint when a step change in load demand is received. From plot (c) it is clear that the FARSMC behaves much better than PI control in that the settling time is dramatically reduced—from more than 80 s to about 20 s.
- The FARSMC's water level control performance (plot d) is also better than that of PI control. The plot indicates that, with FARSMC, the reactor water level fluctuates with about half the magnitude compared with PI control. With FARSMC, the transient lasts about 30 s, whereas the reactor level transient lasts more than 80 s with PI control.

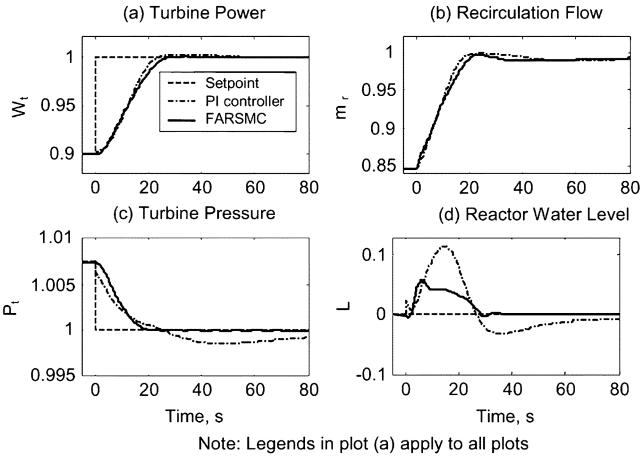

Fig. 6. Plant responses under a step change of $+10\%$ in load demand at 90% rated power.

B. Pressure Setpoint Change

Plant responses to a $+1\%$ step change in pressure setpoint at 72% rated power are shown in Fig. 7. With FARSMC, the transients of turbine throttle pressure (plot d) is similar to that from load demand setpoint change, and the turbine power fluctuation is very minor, almost unnoticeable in plot (a), mainly due to the smooth action of the control valve (plot e). Accordingly, the magnitude of the reactor water level fluctuation (plot f) is also very minor. Compared with FARSMC, the PI controller's performance is not so smooth: the valve abruptly changes its opening with 6% change within 1.5 s (plot e) in response to the pressure setpoint change, resulting in the sharp change in the reactor power (plot b)—the magnitude of the neutron density fluctuation is as high as 9%, and the reactor water lever surges—more than 20% (plot f).

C. Reactor Water Level Setpoint Change

Plant transients under a -10% step change in the reactor water level setpoint were obtained at 100% power level, results of which are shown in Fig. 8. The slow zero-approaching problem of the RSMC raised at the beginning of Section-IV.C has been greatly mitigated with the FARSMC. The reactor water level settling time drops about half, from more than 80 s to about 40 s (plot c). Although the water level change is initially slower with FARSMC than with PI controller, 40 s transient time is reasonable in practice. The feature of the FARSMC is that the level changes very smoothly and there is no undershoot. With PI control, however, water level has an undershoot and still does not reach its final value at 80 s.

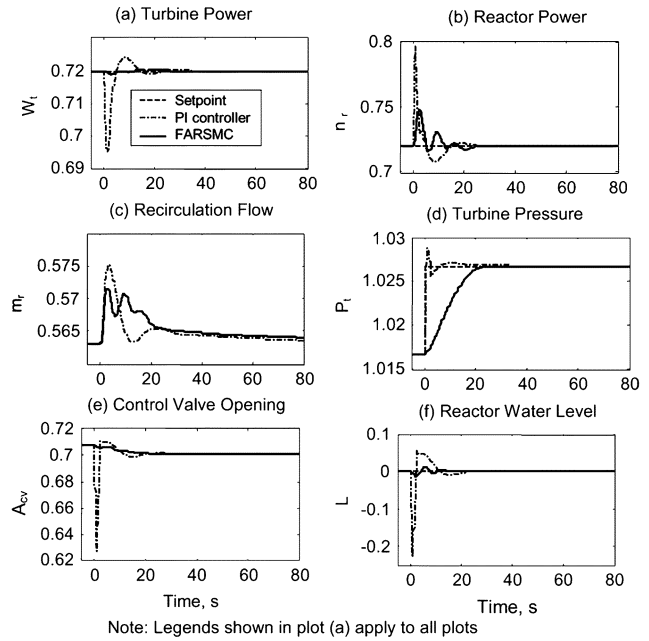

Fig. 7. Plant responses under a step change of $+1\%$ in pressure setpoint at 72% rated power.

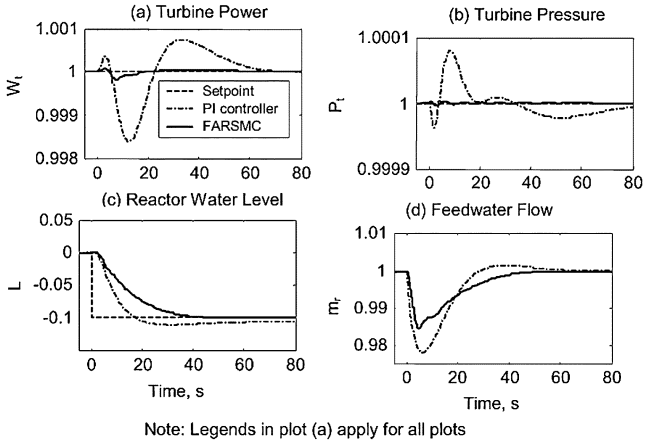

Fig. 8. Plant responses under a step change of -10% in reactor water level setpoint at 100% rated power.

From the transients of other variables, such as the turbine power (plot a), and the throttle pressure (plot b), etc., it is clear that the FARSMC results in smaller-magnitude responses than PI controllers, even though the magnitude of these variable responses with PI controllers are not significant during the reactor water level setpoint change transient.

D. Disturbance of Reactivity Insertion

Shown in Fig. 9 are the simulation results when the reactor receives an inadvertent 0.01$ reactivity insertion as a step input at 90% rated power condition.

From comparison of the responses from PI controllers and from the FARSMC, it is clear that most variables' transients are milder and faster to reach their final values with the FARSMC. The one exception is the neutron density or reactor power (plot c), which is promptly affected by the reactivity insertion in the prompt-jump approximation model. Overall, the designed

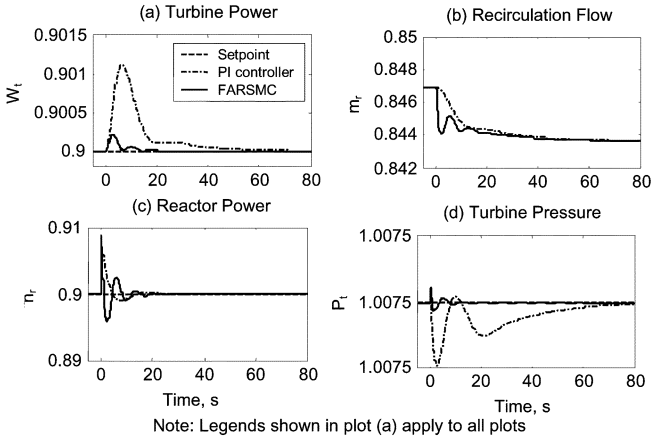

Fig. 9. Plant responses under a 0.01$ reactivity step insertion at 90% rated power.

FARSMC is more robust with respect to the reactivity disturbances.

Shyu and Edwards designed a MIMO robust controller for the same ABWR system as used in this study based on the Jacobian-linearized system [2]. That controller behaves not as well as the PI controller because the system design does not give much room for the system to deal with disturbances. The FARSMC is another type of robust controller directly oriented toward nonlinear systems and it deals with uncertainties in an implicit way by using a recursive algorithm. Unlike linear system robust controller design, which needs to specify the type and magnitude of each uncertainty in advance, the design of FARSMC does not require detailed uncertainty information. Linear system robust control needs painstaking care to acquire this information: overly conservative estimation of uncertainties will not allow any possible robust controller design; on the other hand, underestimation of uncertainties may cause the resulting controller to fail during implementation. This dilemma is avoided in FARSMC design. Therefore, in this sense, the FARSMC has its advantages over the theoretically well-established linear system robust control technique.

VI. Summary and Conclusion

In this study, sliding-mode control technique is employed to design a MIMO controller for an ABWR plant control. In order to avoid the chattering problem encountered with the conventional SMC, the control algorithm is modified into a recursive form, resulting in RSMC. To further improve the performance of the RSMC, fuzzy-adaptation technique is employed to adjust the RSMC parameter based on plant states, resulting in FARSMC, leading to faster yet milder system responses.

The resulting FARSMC has been validated with simulations under various transients, including setpoint step changes in the desired value of each output at different power levels and the disturbance of inadvertent reactivity insertion. All design objectives are achieved under these transients. In comparison with the existing PI controllers, the FARSMC's performances are superior in all cases considered. Specifically, with FARSMC: 1) the control action of turbine throttle valve is significantly milder with less amplitude power and reactor water level fluctuations;

2) settling time of the system pressure is shorter with all setpoint step change transients; 3) during load-demand step-change transients, the reactor water level fluctuates with less amplitude, shorter settling time and zero under/overshoot; and 4) the controller is robust in that it is more capable of rejecting external-disturbance in the case of reactivity insertion.

REFERENCES

[1] K. Zhou, J. Doyle, and K. Glover, *Robust and Optimal Control*. Upper Saddle River, NJ: Prentice-Hall, 1996.

[2] S. Shyu and R. M. Edwards, "A robust multivariable feedforward/feedback controller design for an integrated power control of boiling water reactor power plants," *Nucl. Technol.*, vol. 140, pp. 129–146, 2002.

[3] C. Edwards and S. K. Spurgeon, *Sliding Mode Control: Theory and Applications*. London, U.K.: Taylor Francis, 1998.

[4] K. Erbatur, O. Kaynak, A. Sabanovic, and I. Rudas, "Fuzzy parameter adaptation for a sliding mode controllers as applied to the control of an articulated arm," in *Proc. IEEE Int. Conf. Robotics and Automation*, Albuquerque, NM, Apr. 1997, pp. 817–822.

[5] A. Sabanovic, K. Jezernik, and K. Wada, "Chattering-free sliding modes in robotic manipulators control," *Robotica*, vol. 14, pp. 17–29, 1996.

[6] L.-X. Wang, *A Course in Fuzzy Systems and Control*. Englewood Cliffs, NJ: Prentice-Hall, 1997.

[7] Y.-R. Hwang and R. Tomizuka, "Fuzzy smoothing algorithms for variable structure systems," *IEEE Trans. Fuzzy Syst.*, vol. 2, no. 4, pp. 277–289, 1994.

[8] O. Kaynak, K. Erbatur, and M. Ertugrul, "The fusion of computationally intelligent methodologies and sliding-mode copntrol—A survey," *IEEE Trans. Indust. Electron.*, vol. 48, no. 1, pp. 4–17, 2001.

[9] Y. B. Shtessel, "Sliding mode control of the space nuclear reactor system," *IEEE Trans. Aerosp. Electron. Syst.*, vol. 34, no. 2, pp. 579–589, 1998.

[10] D. Ruan, "R&D on fuzzy logic applications at SCK • CEN," in *Proc. Fuzzy Information Processing Society—Biennial North American Conf.*, Berkeley, CA, June 19–22, 1996, pp. 428–432.

[11] Z. Huang and R. M. Edwards, "Sliding-mode control application in ABWR plant pressure regulation," in *Proc. Int. Congress Advanced Nuclear Power Plants (ICAPP) Embedded Int. Topical Annu. Meeting 2002 ANS*, Hollywood, FL, June 9–13, 2002.

[12] H. Temeltas, "A fuzzy adaptation technique for sliding-mode controllers," in *Proc. IEEE Int. Symp. Industrial Electronics*, vol. 1, Pretoria, South Africa, 1998, pp. 110–115.

[13] Z. Huang, K. Y. Lee, and R. M. Edwards, "Fuzzy logic control for nuclear power plant overall control," in *Proc. 15th IFAC World Congress*, Barcelona, Spain, July 21–26, 2002. paper #1392.

[14] Z. Huang, "Fuzzy Adapted Sliding-Mode Controller Design for a Nuclear Power Plant," Ph.D. dissertation, Dept. Mech. Nucl. Eng., Pennsylvania State University, University Park, PA, 2002.

[15] J.-J. E. Slotine and W. Li, *Applied Nonlinear Control*. Englewood Cliffs, NJ: Prentice-Hall, 1997.